Variability of the Winter Wind Waves and Swell in the North Atlantic and North Pacific as Revealed by the Voluntary Observing Ship Data

SERGEY K. GULEV

P. P. Shirshov Institute of Oceanology, Moscow, Russia, and IFM-GEOMAR, Kiel, Germany

VIKA GRIGORIEVA

P. P. Shirshov Institute of Oceanology, Moscow, Russia

(Manuscript received 11 October 2005, in final form 20 March 2006)

ABSTRACT

This paper analyses secular changes and interannual variability in the wind wave, swell, and significant wave height (SWH) characteristics over the North Atlantic and North Pacific on the basis of wind wave climatology derived from the visual wave observations of voluntary observing ship (VOS) officers. These data are available from the International Comprehensive Ocean–Atmosphere Data Set (ICOADS) collection of surface meteorological observations for 1958–2002, but require much more complicated preprocessing than standard meteorological variables such as sea level pressure, temperature, and wind. Visual VOS data allow for separate analysis of changes in wind sea and swell, as well as in significant wave height, which has been derived from wind sea and swell estimates. In both North Atlantic and North Pacific midlatitudes winter significant wave height shows a secular increase from 10 to 40 cm decade^{-1} during the last 45 yr. However, in the North Atlantic the patterns of trend changes for wind sea and swell are quite different from each other, showing opposite signs of changes in the northeast Atlantic. Trend patterns of wind sea, swell, and SWH in the North Pacific are more consistent with each other. Qualitatively the same conclusions hold for the analysis of interannual variability whose leading modes demonstrate noticeable differences for wind sea and swell. Statistical analysis shows that variability in wind sea is closely associated with the local wind speed, while swell changes can be driven by the variations in the cyclone counts, implying the importance of forcing frequency for the resulting changes in significant wave height. This mechanism of differences in variability patterns of wind sea and swell is likely more realistic than the northeastward propagation of swells from the regions from which the wind sea signal originates.

1. Introduction

Ocean wind waves can effectively characterize climate change. Being generated by surface winds, they do not necessarily mirror variability patterns of wind speed. For instance, swell integrates wind properties over the larger scales than the wind sea does. Therefore, changes in significant wave height (SWH) can be affected by both local and remote wind forcing. Moreover, storminess has a profound impact on operations of marine carriers and logistics of marine structures. Thus, the analysis of climate variability in wind wave characteristics is crucially important for the minimization of risks of these activities. The four major sources of global wind wave observations are in situ time series, long-term model hindcasts, satellite altimeter measurements, and voluntary observing ship (VOS) data. Each of these can be used for the estimation of climate variability in wave parameters. Carter and Draper (1988) and Bacon and Carter (1991, 1993) from the 16-yr time series recorded at the Seven Stones Light Vessel (SSLV) and Ocean Weather Station (OWS) L reported about 1% yr^{-1} secular growth of SWH in the northeast Atlantic from the late 1960s to the early 1980s. Analysis of in situ time series at the National Data Buoy Center (NDBC) buoys in the northeast Pacific (Allan and Komar 2000; Gower 2002) showed upward trends of 12–27 cm decade^{-1} in annual mean SWH, with winter (October–March) trends being from 21 to 42 cm decade^{-1} during the period of 1978–99. These changes were also confirmed by the long-term estimates of storminess de-

Corresponding author address: Sergey Gulev, P. P. Shirshov Institute of Oceanology, RAS, 36 Nakhimovsky Ave., 117851 Moscow, Russia.
E-mail: gul@sail.msk.ru

rived from the tide gauge residuals (Bromirski et al. 2003). However, buoy measurements are available in a few locations only and cover the period from the late 1970s onward.

In this context global wave hindcasts simulated by the advanced wave models driven by the reanalysis winds are particularly attractive. After the first climate analysis of manual wave charts (Neu 1984), Kushnir et al. (1997), Sterl et al. (1998), and the WASA group (1998; Günther et al. 1998; Bauer and Staabs 1998) performed the first model-based analyses of climate variability of SWH in the North Atlantic. These results have shown an increase of the North Atlantic SWH from the mid-1950s to the mid-1990s. Hindcasts of Cox and Swail (2001), Wang and Swail (2001, 2002), and Sterl and Caires (2005) based on National Centers for Environmental Prediction–National Center for Atmospheric Research (NCEP–NCAR) and the European Centre for Medium-Range Weather Forecasts (ECMWF) 40-yr Re-Analyses (ERA-40) winds show a growing mean SWH as well as an intensification of SWH extremes during the last 40 yr. In particular, the 99% extreme of the winter SWH increased in the northeast Atlantic by a maximum of 0.4 m decade^{-1} (Wang and Swail 2001; Caires and Sterl 2005a). However, centennial hindcasts for the twenty-first century, based on the forcing reconstructed from the observed relationships between sea level pressure (SLP) and SWH (Wang et al. 2004; S. Caires and A. Sterl 2005, personal communication), show different signs of trends in SWH extremes for different scenarios and different seasons. Models can also reveal regional changes in wind wave characteristics. Vikebo et al. (2003) demonstrated growing SWH in the northern North Atlantic using a 118-yr wave hindcast of the Norwegian Meteorological Institute (DNMI). For the same region Weisse et al. (2005) reported a growing number of independent storms in the northeast Atlantic, as simulated by a regional climate model. Similarly, growing storminess in the North Pacific has been demonstrated by Graham and Diaz (2001).

However, the model wave hindcasts are constrained by the model performance and the wind forcing used. Thus, inhomogeneities in reanalysis winds can influence the patterns of climate variability in the wave hindcasts. These inhomogeneities were primarily identified in the Southern Hemisphere where they are associated with the changing data assimilation input (Sterl 2004). However, there were also changes in the amount of assimilated data (first of all satellites) in the Northern Hemisphere (Kistler et al. 2001; Uppala et al. 2005). Caires and Sterl (2005b) and Sterl and Caires (2005) compared ERA-40 Numerical Wave Model (WAM) hindcast with buoy and altimeter data in the northeast Pacific and northwest Atlantic. They argued that at least for the two periods in the 1990s, assimilation of the Fast Delivery Products (FDP) from the *European Remote Sensing Satellite* (*ERS*)*-1*/*-2* affected the homogeneity of wind and wave time series. Swail et al. (1999) demonstrated that trends in wind speed from NCEP–NCAR reanalysis and high-quality measurements at OWS B and P as well as at Sable Island (SI) may exhibit quantitative differences, being qualitatively comparable. Satellite data recently also started to provide global time series of wind wave characteristics for the period from 1 to 2 decades. For instance, Woolf et al. (2002) reported increases of SWH in the North Atlantic midlatitudes from a 14-yr (1988–2002) time series of the merged Ocean Topography Experiment (TOPEX)/Poseidon and *ERS-1*/*-2* Ku-band altimeter data. Although generally sparse sampling provided by individual satellites can be improved by combining tracks from different spacecrafts, this procedure requires intercalibration of instruments on board different satellites (Challenor and Cotton 2003). Nevertheless, despite some limitations in the coastal regions (Woolf et al. 2003), these data cover the globe with quite homogeneous sampling and in the future will become superior with respect to the VOS data. However, at present these data are still short to be extensively applied for climate variability studies. Moreover, satellite altimeters report SWH exclusively and do not provide separate estimates of sea and swell.

VOS wave data provide visual estimates of wave parameters, reported by marine officers worldwide starting from 1856 (Worley et al. 2005; Gulev et al. 2003a; Gulev and Grigorieva 2004). In comparison to the other sources, these data have the longest record and provide independent estimates of wind sea and swell. Limited collections of these data were used for the development of wave statistics for marine officers and naval engineers (Hogben and Lumb 1967; Hogben et al. 1986) and global and regional climate summaries (Naval Oceanography Command Detachment 1981; Paskausky et al. 1984; Korevaar 1990). Analysis of climate variability based on these data was for a long time limited to the consideration of the OWS subsets (Walden et al. 1970; Rodewald 1972; Rye 1976). More extensive use of these data for climate research requires correction of many biases and minimization of observational errors inherent to visual observations (Houmb et al. 1978; Jardine 1979; Dacunha et al. 1984; Laing 1985; Soares 1986; Hogben et al. 1983; Hogben 1988; Wilkerson and Earle 1990; Hogben and Tucker 1994; Gulev et al. 2003a,b). Gulev and Hasse (1998) first derived the 30-yr (1964–93) North Atlantic climatology of visual wind

waves based on the most complete collection of VOS observations, known now as International Comprehensive Ocean–Atmosphere Data Set (ICOADS; Worley et al. 2005). Gulev et al. (1998) validated this product against altimeter data, and a numeric wave model hindcast of Sterl et al. (1998). Gulev and Hasse (1999) used these data for the analysis of secular wave changes in the North Atlantic and have shown growing SWH and swell in the northeast Atlantic; however, that was not the case for the wind sea driven by the local winds.

Recently Gulev et al. (2003a) developed a global climatology of VOS wind waves now spanning the period of 1958–2002. This product was accompanied by an extensive analysis of all sources of uncertainties inherent to visual observations of waves. Gulev and Grigorieva (2004) used the full ICOADS collection and developed 120-yr-long homogenized time series of SWH for the well-sampled locations of major ship routes. Analysis has shown significantly positive trends in annual mean SWH almost everywhere in the North Pacific, with a maximum trend of 8–10 cm decade^{-1} (0.5% yr^{-1}) and weak negative trends along the North Atlantic storm track. During the period of 1958–2002, linear trends in annual mean SWH were significantly positive over most of the North Atlantic and North Pacific with the largest upward changes of 14 cm decade^{-1}. However, the study of Gulev and Grigorieva (2004) was concentrated on centennial changes and was limited to the analysis of trends in SWH, because visual data do not provide separate estimates of wind sea and swell prior 1950s. In this work we focus on the interannual- to decadal-scale variability in wind sea and swell, which are massively available after the late 1950s only. We will analyze trends and interannual variability in the characteristics of wind sea and swell in the Northern Hemisphere oceans primarily during the winter season, using the VOS-based wave climatology of Gulev et al. (2003a), extended to 2002.

2. Data and preprocessing details

A global climatology of wind wave characteristics (Gulev et al. 2003a) has been developed on the basis of the latest update of the ICOADS collection of marine meteorological observations (Worley et al. 2005) and the guidelines for the preprocessing of visual wave data developed by Gulev and Hasse (1998) and Gulev et al. (2003a,b). A comprehensive description of the data processing, coding systems, changes in data formats, ad hoc corrections of biases, and estimates of the uncertainties can be found in Gulev et al. (2003a). In this article we consider the variability of wind sea height (h_w), swell height (h_s), and SWH. The major biases in these parameters, which have been considerably reduced in the climatology of Gulev et al. (2003a), were the overestimation of small wave heights and poor separation of wind sea and swell. Gulev et al. (2003a) also provided global estimates of random observational errors in h_w and h_s, estimates of day–night differences, and estimates of sampling uncertainties. Sampling errors were found to be large in the poorly sampled Southern Ocean, where they dominate over the other error sources. For this reason we analyze in this study climate variability only in the North Atlantic and North Pacific, which are characterized starting from the late 1950s by quite homogeneous sampling. The values of SWH are not directly reported by VOS, but should be computed from the visual estimates of wind sea and swell heights. Gulev et al. (2003a) provide estimates of SWH, which were derived from a combined approach first suggested by Barratt (1991) and later modified by Gulev and Hasse (1998). This approach suggests the use of the theoretical definition (square root of the sum of squares of wind sea and swell heights) only for the cases when wind sea and swell are within the same 30° directional sector and taking the maximum of the two components in all other cases,

$$\mathrm{SWH} = \begin{cases} (h_w^2 + h_s^2)^{1/2}, & [\mathrm{dir_{sea}}, \mathrm{dir_{swell}}] \in 30^\circ \text{ sector} \\ \max[h_w, h_s], & [\mathrm{dir_{sea}}, \mathrm{dir_{swell}}] \notin 30^\circ \text{ sector} \end{cases}. \quad (1)$$

Gulev et al. (2003a) analyzed different algorithms of the computation of SWH. Although climatological deviations between different SWH estimates may amount to 0.3 m, different methods do not imply any significant differences in variability patterns.

Climatology of wind wave parameters used here (Gulev et al. 2003a) has monthly resolution in time and 2° × 2° resolution in space covering the world oceans from 80°S to 80°N. Monthly gridded values were obtained by the averaging of individual wave parameters within 2° × 2° boxes using the 4.5-σ trimming limits for the estimation of monthly mean wave parameters. This limit has been applied instead of the traditionally used 3.5-σ limit. The latter may not necessarily effectively distinguish between outliers and extreme values and thus implies biases in the monthly time series (e.g., Wolter 1997). Spatial interpolation into unsampled locations and spatial smoothing of monthly fields were provided by the modified method of local procedures (Akima 1970) in combination with two-dimensional elliptic Lanczos filtering (Lanczos 1956; Duchon 1979). In this sense the climatology represents a typical state-of-the-art VOS-based product, similar to the climatology of air–sea flux and flux-related variables (e.g., da Silva et al. 1994; Josey et al. 1999). In this study we used

seasonal wintertime series derived from the monthly gridded values for January–March (JFM) for the 45-yr period from 1958 to 2002 over the North Atlantic and North Pacific.

For the association of the wave height variability with the atmospheric circulation characteristics we used wind speed and characteristics of atmospheric cyclone activity. Monthly 2° fields of surface wind speed have been derived from the ICOADS reports for the period of 1958–2002. ICOADS winds are known to be influenced by time-dependent biases, which cause significant upward trends (up to 40 cm s^{-1} $decade^{-1}$) of an artificial nature. These trends are not supported by the evidence from island stations (Ramage 1984; Schmidt and von Storch 1993), surface pressure gradient data (Ward 1992; Ward and Hoskins 1996), and alternative marine meteorological observations (Isemer 1995). The biases are associated with the changing ratio between the anemometer measurements and Beaufort wind estimates (Peterson and Hasse 1987; Cardone et al. 1990), historical changes in the usage of equivalent scales (Lindau et al. 1990; Lindau 2006), and the inaccurate evaluation of the true wind speed from the relative wind (Gulev 1999). To minimize these biases, we used only the wind speed reported in the same reports as the wave information. All Beaufort estimates were converted from the WMO1100 equivalent scale (WMO 1970) to the least biased Lindau (1995, 2006) equivalent scale, as recommended by Kent and Taylor (1997). All anemometer measurements starting from 1973 were adjusted to 10-m measurement height using the WMO-47 "International list of selected, supplementary and auxiliary ships" (WMO 1973; Kent et al. 2006), when available. When no information on the anemometer heights was available as well as for the period prior 1973 (no availability of WMO-47 document) the defaults from Josey et al. (1999) were applied to ships and platforms. However, even this preprocessing still may not necessarily remove all artificial signals. Thus, we will limit our analysis of the wind speed to interannual variability in the detrended time series for the period of 1958–2002. We do expect that interannual- to decadal-scale signals are quite reliable in the wind speed data used.

Variability in atmospheric cyclone activity was quantified using the results of the storm tracking performed for the period from 1958 to 2002 on the basis of the 6-hourly NCEP–NCAR reanalysis SLP fields. Cyclone trajectories were produced using a numerical scheme, developed on the basis of the archive of storm tracks for the 42 winter seasons (1958–99) (Gulev et al. 2001; Grigoriev et al. 2000). The numerical scheme generally follows the method of Murray and Simmonds (1991), but includes dynamic interpolation of the SLP fields and shows very good agreement with the results of semimanual tracking of Gulev et al. (2001). The output of the tracking (coordinates, time, and corresponding SLP values) was used to locate cyclone trajectories and to compute cyclone numbers and frequencies for 5° cells. For this purpose we used the mapping procedure of Zolina and Gulev (2002), minimizing the biases in cyclone counts for the latitude–longitude cells.

3. Secular changes in wind wave heights

We start with the analysis of secular tendencies in the winter characteristics of wind waves. Gulev and Grigorieva (2004), for the period of 1958–2002, demonstrated strong upward changes of up to 14 cm $decade^{-1}$ in the annual mean SWH in the northwest Atlantic and northeast Pacific and argued that these changes were largely dominated by the winter tendencies. Figure 1 shows estimates of linear trends in the winter (JFM) wind sea height, swell height, and SWH, together with their statistical significance in the North Atlantic and North Pacific. Statistical significance was estimated according to a Student's t test and was additionally analyzed using the Hayashi (1982) reliability ratio (H), which considers the confidence intervals of the statistical significance. If $|H| \gg 1$, the true value is close to its estimate. When $|H| \leq 1$, confident intervals can be quite wide, even if the Student's t test is formally satisfied.

During the winter season the largest upward changes in the wind sea height (Fig. 1a) are observed in the central Atlantic midlatitudes, in the Norwegian Sea (up to 30 cm $decade^{-1}$), and in the western tropical Atlantic (from 5 to 15 cm $decade^{-1}$). However, in the northeast Atlantic wind sea height shows the area of statistically significant negative trends from -10 to -20 cm $decade^{-1}$. Trends in the swell height show strong upward changes in the eastern subpolar North Atlantic and in the Norwegian Sea with a maximum of 38 cm $decade^{-1}$. Relatively weak statistically significant negative trends of swell height (less than 10 cm $decade^{-1}$) were found in the central subtropics and the Gulf of Mexico. Resulting upward tendencies in SWH amount to 0.4 m $decade^{-1}$ (1% yr^{-1}) in the central subpolar Atlantic and Norwegian Sea (Fig. 1c), where both wind sea and swell indicate secular increasing. At the same time, in the eastern midlatitudinal Atlantic trends in SWH are somewhat weaker than those in swell height, being influenced by the negative changes in the wind sea height (Fig. 1a). Figure 2a shows winter time series of wind wave parameters averaged over the region 54°–64°N, 10°–20°W, where instrumental records of Bacon and Carter (1991, 1993) reported secularly growing SWH by approximately 1% yr^{-1}. Our results support positive

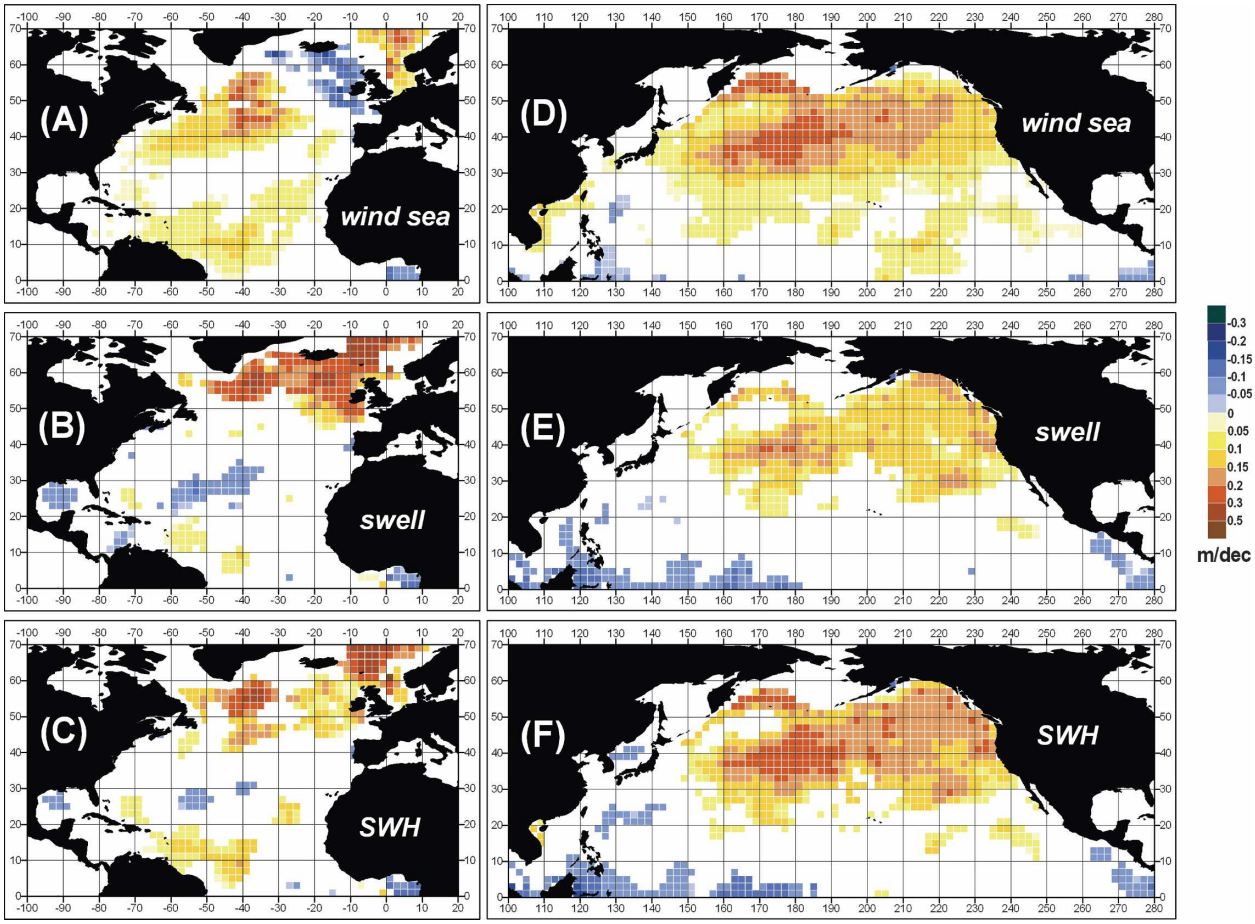

FIG. 1. Linear trends (m decade^{-1}) in winter (JFM) (a), (d) wind sea height, (b), (e) swell height, and (c), (f) SWH for the (a)–(c) North Atlantic and (d)–(f) North Pacific. Only trends significant at 95% level and according to Hayashi criterion are shown.

trends in SWH. This change is largely provided by growing swell and not by the wind sea, which alternatively shows here weak negative changes. Weak negative trends in all wave components are observed in the eastern equatorial Atlantic, where h_w decreases by 5–15 cm decade^{-1} (0.4%–1.1% yr^{-1}).

Patterns of the winter linear trends in the North Pacific wind sea height, swell height, and SWH (Figs. 1d–f) are more consistent with each other than in the North Atlantic. A large area of the growing wave height aligns along the North Pacific midlatitudinal storm track. The largest linear trends in h_w (exceeding 0.2 m decade^{-1}) are observed in the central midlatitudinal Pacific approximately at 37°N, 175°E. Trends in the swell height are somewhat weaker and range from 10 to 15 cm decade^{-1} in most locations with the strongest upward tendency of 20 cm decade^{-1} at 40°N, 179°E. In the eastern midlatitudinal Pacific the pattern of the swell trends is somewhat shifted to the northeast with respect to the wind sea and forms the local maxima of SWH changes along the U.S. coast, reflecting the propagation effect of swell. The pattern of the linear trends in SHW (Fig. 1f) represents the joint effect of wind sea and swell changes and shows the largest increase of 0.30 m decade^{-1} in the eastern Pacific midlatitudes and subpolar regions. Figure 2b shows time series of the wave parameters averaged over the northeast Pacific (44°–54°N, 142°–154°E). In this region buoy records report growing SWH from the 1970s to 1990s (Allan and Komar 2000; Gower 2002). Figure 2b shows more consistent changes in the wind sea, swell, and SWH than in the North Atlantic, indicating, however, some differences in the behavior of wind sea height and swell height on interdecadal time scales. During the period from the late 1950s to the early 1970s wind sea height does not show any significant upward tendency, but swell height increases strongly by approximately 90 cm during the 15-yr period. Alternatively, starting from the mid-1970s, wind sea goes up by more than 20 cm decade^{-1} while swell height demonstrates a very weak secular change

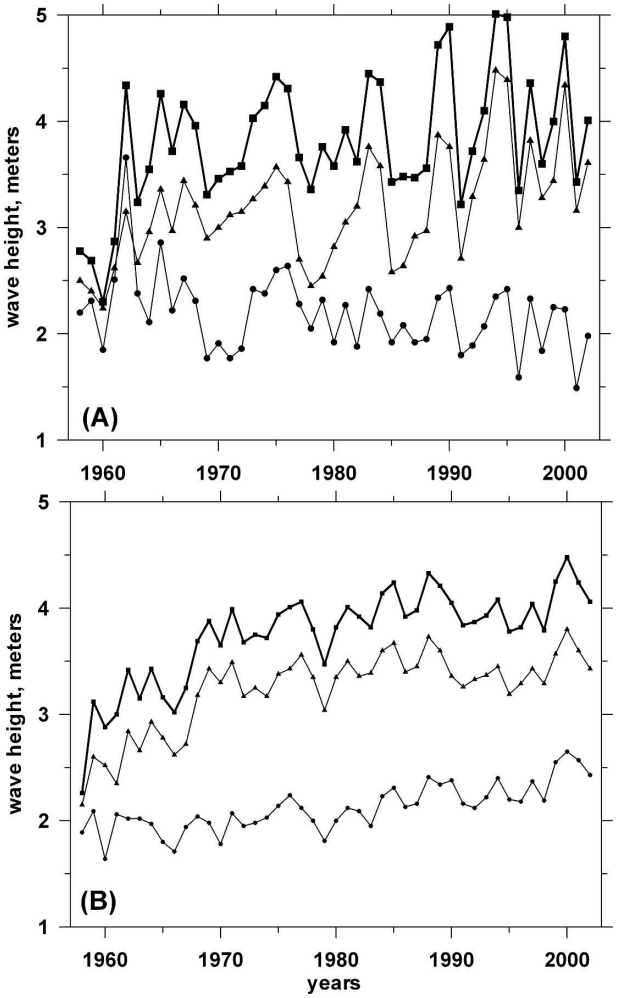

FIG. 2. Time series of winter wind sea height (circles), swell height (triangles), and SWH (squares) averaged over the areas (a) 54°–64°N, 10°–20°W in the Atlantic and (b) 44°–54°N, 142°–154°E in the Pacific.

for this period. This implies that the trend in SWH is primarily implied by the secular changes in swell during the period from the late 1950s to mid-1970s and by wind sea change in the later decades. Significantly negative trends, from -0.1 to 0.15 m decade^{-1}, in the Pacific swell height and SWH are observed in both western and eastern equatorial regions.

Our estimates can be compared with seasonal trends in SWH for the period of 1958–2001 of Caires and Swail (2004). These were derived from the ERA-40 WAM wave hindcast, corrected for temporal inhomogeneities (Caires and Sterl 2005b). They report the highest positive trends of 0.24 m decade^{-1} in the North Pacific and 0.26 m decade^{-1} in the North Atlantic. These estimates are qualitatively consistent with those of Wang and Swail (2006), derived for the period of 1958–97 from the Cox and Swail (2001) dataset. Our strongest positive trends in SWH in the North Pacific (0.29 m decade^{-1}) are somewhat higher than those of Caires and Swail (2004). In the North Atlantic our trends in SWH are approximately 50% higher than those reported by Caires and Swail (2004). Qualitatively similar conclusions can be drawn from the comparison with the analysis of Sterl and Caires (2005), who presented February trends in SWH in the same dataset. Our trends in the northeast Pacific are in a qualitative agreement with Allan and Komar (2000) and Gower (2002) estimates for the period from the late 1970s to the late 1990s derived from the in situ buoy data. Quantitative comparison shows that our estimates are somewhat weaker than those reported by buoys that can be explained by the spatial averaging in a gridded product. Wave data from satellite altimetry (Cotton et al. 2003; Woolf et al. 2002) provide relatively short time series. Comparison with them reveals quite good agreement of interannual variability and trends during the late 1980s and 1990s (Gulev et al. 1998). For instance, for the northeast Atlantic Cotton et al. (2003) reported an increase of more than 0.5 m in SWH between the pentades of 1985–89 and 1991–95. Our data show a 10%–20% smaller increase (0.43 m) with the pattern of differences being very comparable to that of Cotton et al. (2003).

Summer linear trends (not shown) are quite weak in both the North Atlantic and North Pacific and show statistically significant positive changes of 3–6 cm decade^{-1} in the subtropics of both oceans and weak negative changes in the Tropics. This implies that secular changes in the annual mean SWH, at least in the midlatitudinal and subpolar regions, considered in many model and experimental studies, are largely influenced by the winter tendencies. To quantify the persistency of the trend characteristics during the annual cycle we show in Fig. 3 the seasonal cycle in the trend estimates in percent per decade (with respect to the decadal mean of 1958–67) computed using monthly mean wind sea and swell heights along the two longitudes in the eastern Atlantic and eastern Pacific. Trends in the wind sea height in the northeast Atlantic north of 50°N are significantly negative during the whole year except for April, with the strongest absolute downward tendencies in February–March and the strongest relative change in winter and summer. In the midlatitudes and northern subtropics significantly positive secular tendencies are observed during spring and autumn with the strongest relative change of about 10% decade^{-1} in October–December. Seasonality in the swell height trends is evident in the subpolar eastern North Atlantic where the positive trends are observed in winter and the negative changes are identified during the late summer. Midlati-

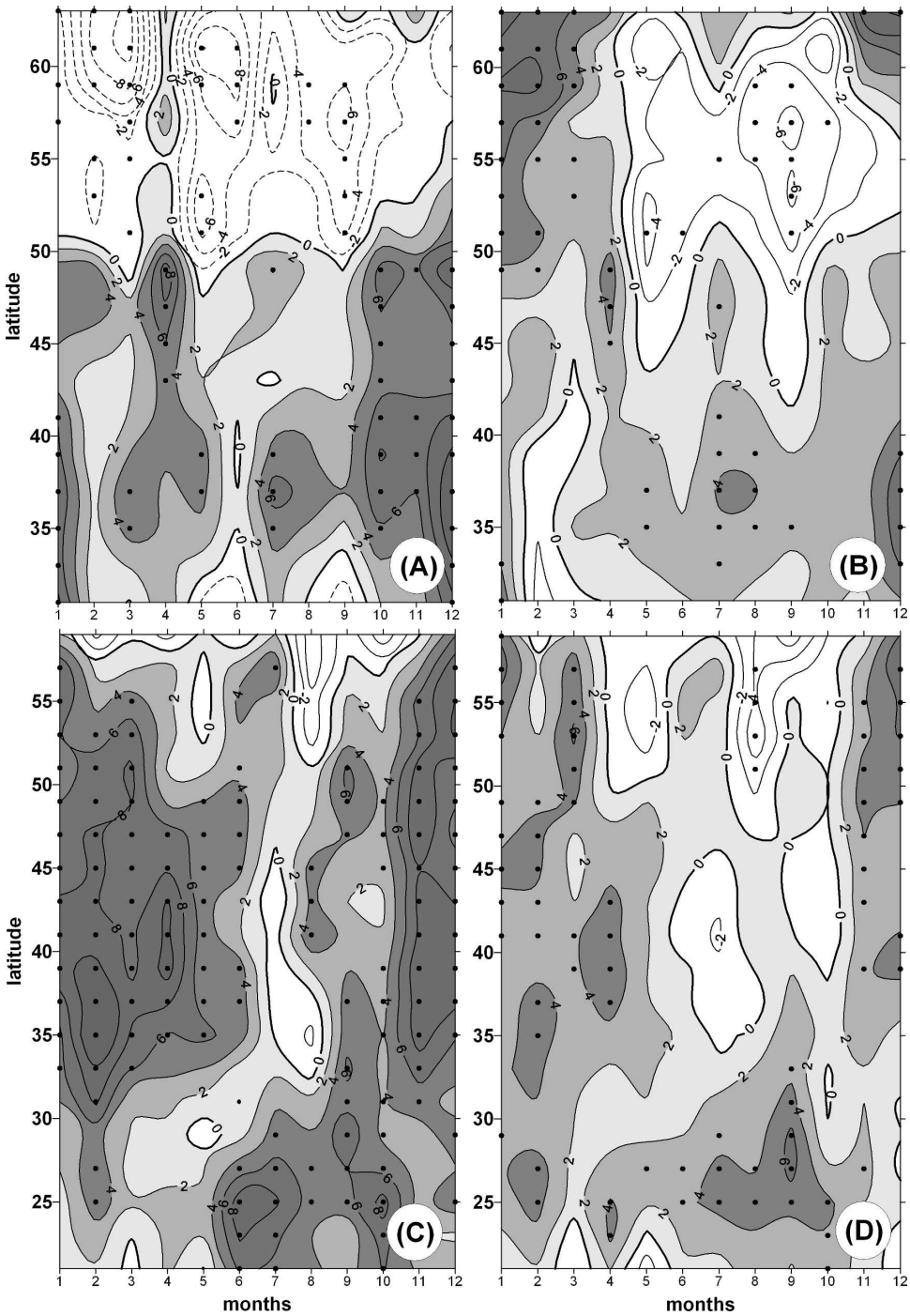

FIG. 3. Seasonal evolution of the monthly linear trends (% decade^{-1}) in (a), (c) wind sea height and (b), (d) swell height for the meridional sections along (a), (b) 20°W in the Atlantic and (c), (d) 150°E in the Pacific. Trends that are significant at the 95% level and according to Hayashi criterion are indicated by black circles.

tudinal trends in swell height demonstrate much more persistency during the year, being primarily positive with the strongest relative change in summer. Similar diagrams for the North Pacific (Figs. 3c,d) imply much stronger seasonal persistency of the linear trends of the wind sea height at all latitudes. The strongest absolute and relative changes are observed during winter and autumn, exceeding 12% decade^{-1} at 35°–40°N. The

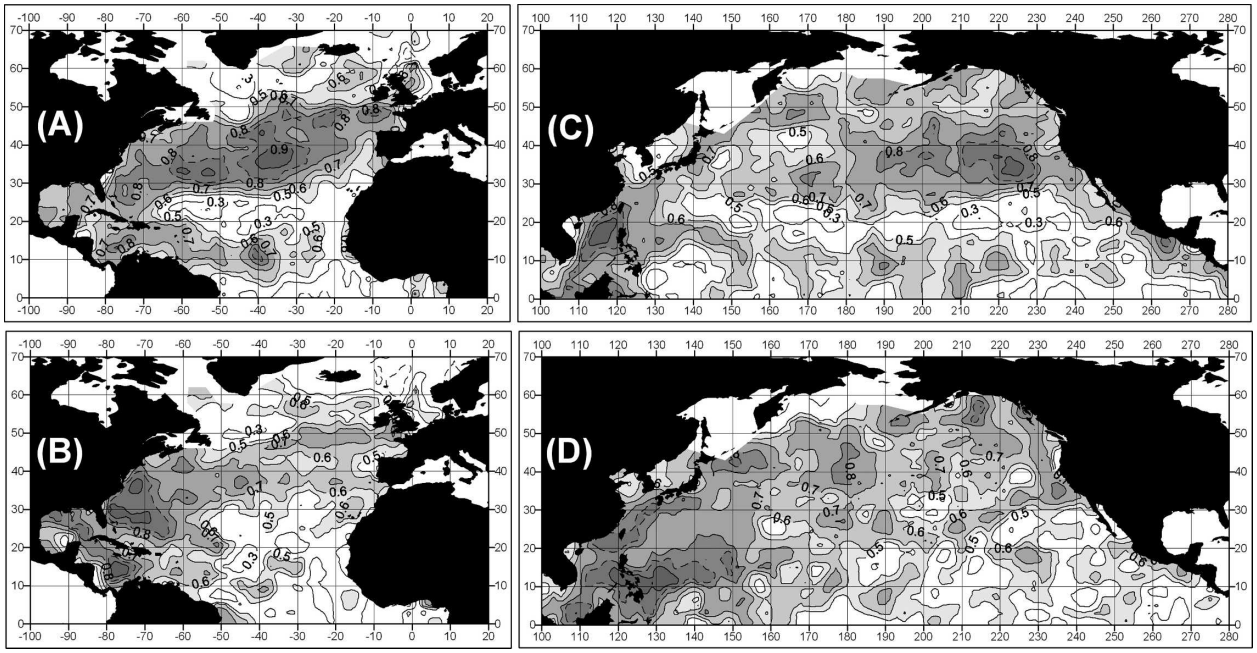

FIG. 4. (a), (c) Winter and (b), (d) summer correlation between the detrended anomalies of wind sea and swell height in the (a), (b) North Atlantic and (c), (d) North Pacific.

swell diagram is qualitatively quite similar to that for the wind sea with the highest secular changes in the midlatitudes during winter and autumn.

4. Interannual variability in the wind wave heights

Figure 2 already implies noticeable differences in the character of the interannual variability of different wave components. Thus, in the northeast Atlantic (Fig. 2a), decadal-scale changes primarily dominate in the variability of swell height, while wind sea variability is characterized by more pronounced shorter period interannual variations. In the northeast Pacific, time series of wind sea and swell heights (Fig. 2b) are better correlated with each other. Figure 4 shows winter and summer local correlations between the detrended anomalies of wind sea height and swell height in the North Atlantic and North Pacific. The highest correlation exceeding 0.9 is observed in winter in the central subtropical Atlantic and in the northeastern subtropical Pacific. During the summer season the largest correlations (>0.9) are observed in the western parts of both oceans, including subtropical semienclosed seas, where the swell fetches are limited and swell typically originates from the same synoptic systems as does the wind sea. However, in the subpolar North Atlantic and in the eastern midlatitudinal Pacific correlation coefficients are smaller than in the western parts of the oceans. They range from 0.3 to 0.7 in the Atlantic and from 0.4 to 0.75 in the Pacific, implying that on average only less than 60% of variability in swell height can be explained by the collocated changes in wind sea in these areas. In the eastern parts of the oceans wind sea is forced by the local wind, while swell is largely dominated by the signals propagating from the west. This is particularly pronounced in the Atlantic subpolar latitudes and in Norwegian Sea, where correlation drops in many locations lower than 0.3 (95% significance level for our time series). Although in both basins swell integrates the wind properties over the larger domain than the wind sea does, in the subpolar Pacific these scales are likely closer to each other. Thus, we can expect that differences between the patterns of interannual variability of wind sea and swell will be the largest in the subpolar North Atlantic latitudes.

To analyze the structure of interannual variability in wind sea, swell, and SWH we applied EOF analysis to the detrended winter time series. Figure 5 shows spatial patterns of the first EOFs of wind sea height, swell height, and SWH for both basins. In the North Atlantic the first EOF accounts for 28%, 33%, and 30% of the total variance for wind sea height, swell height, and SWH, respectively. The corresponding percentages for the North Pacific give 23%, 26%, and 25%. Spatial patterns of the leading modes of h_w, h_s, and SWH are qualitatively comparable with each other in both basins. In the Atlantic they are formed by the anomalies of one sign in the subpolar latitudes and Tropics and the anomalies of the opposite sign in the subtropics.

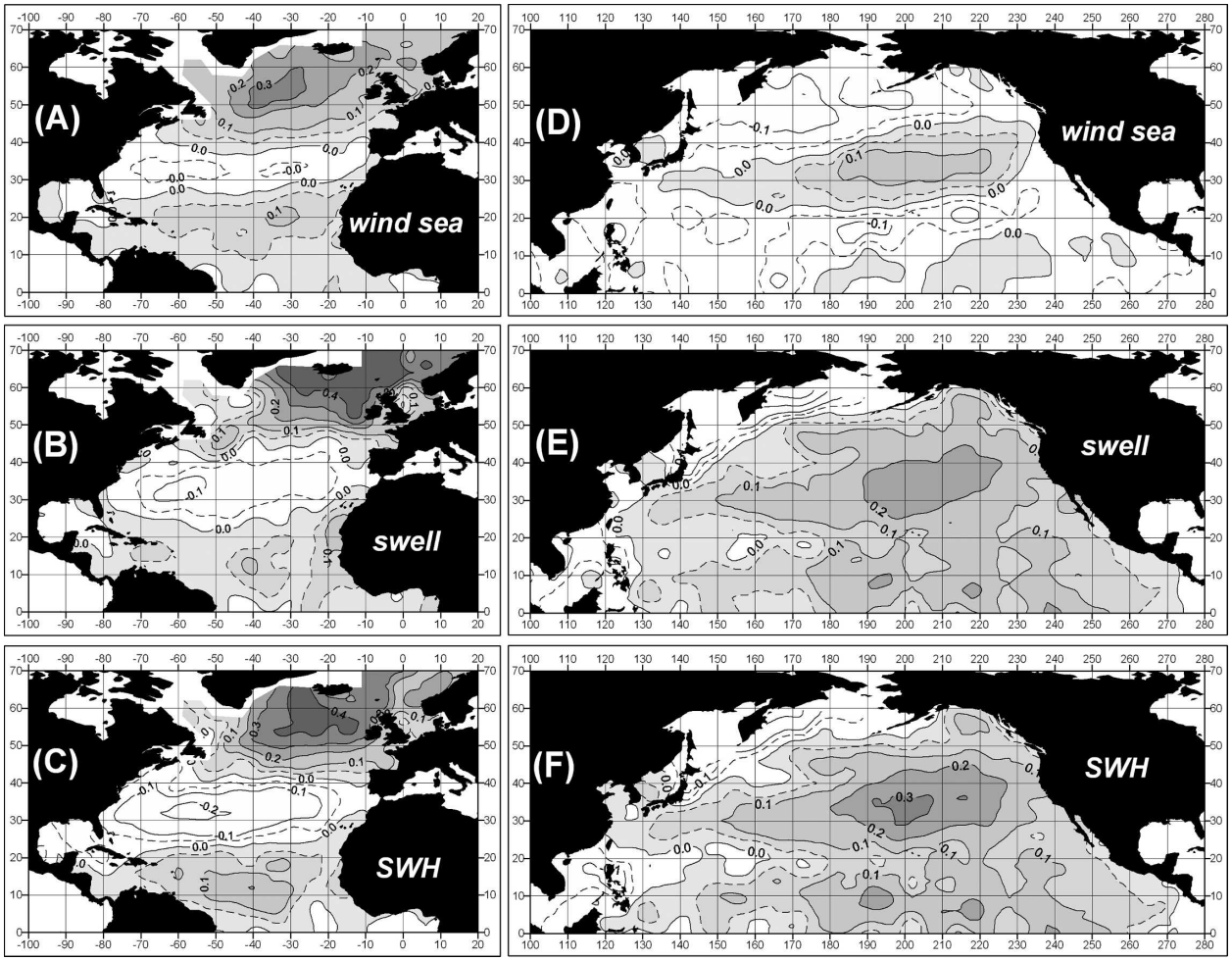

FIG. 5. First EOFs of winter detrended (a), (d) wind sea height, (b), (e) swell height, and (c), (f) SWH in the (a)–(c) North Atlantic and (d)–(f) North Pacific.

Nevertheless, we found some noticeable differences between spatial patterns of wind sea, swell, and SWH in the Atlantic Ocean. Thus, the maximum explained variance for the wind sea is observed in the central subpolar North Atlantic at approximately 50°–60°N, while the northern center of action of the swell height pattern has two maxima of explained variance, of which one is shifted eastward in the northern European basin and Norwegian Sea and another is located in the Greenland–Iceland–Norwegian (GIN) Sea southeast of Greenland. The resulting pattern of SWH (Fig. 5c) is characterized by the northern maximum of explained variance at approximately 57°N, 25°E. The first EOF patterns of swell height and SWH in the western Pacific are characterized by the anomalies of the opposite sign with respect to the central and eastern Pacific (Figs. 5e,f). The wind sea anomalies of the opposite sign are observed in the northwestern subpolar regions and in the southeastern Tropics (Fig. 5d). Note that the magnitude of interannual variability of all wave components is 20%–50% stronger in the Atlantic than in the Pacific. This is also evident from the time series in Fig. 2. Leading modes of interannual variability of swell, shown in Fig. 5b, reveal much more similarity with the linear trend pattern (Fig. 1b) than the interannual mode of the wind sea. In general, in both the Atlantic and Pacific the areas of the strongest trends are somewhat shifted to the west with respect to the areas of the strongest interannual variability.

Figure 6 shows the first normalized principal components (PCs) corresponding to the EOF patterns displayed in Fig. 5. Table 1 shows the correlation coefficients between the first PCs of different wave height components with each other and with the North Atlantic Oscillation (NAO) index (Hurrell 1995) for the whole 45-yr period and the periods of 1958–79 and 1980–2002. In the North Atlantic the leading modes of the wind sea and swell heights are not highly correlated

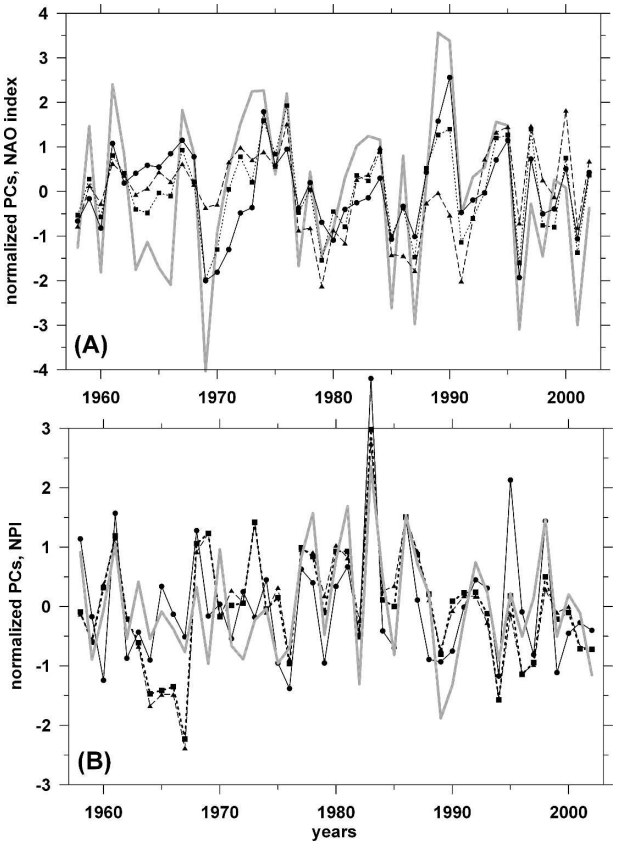

FIG. 6. First normalized PCs of winter detrended wind sea height (circles), swell height (triangles), and SWH (squares) in the (a) North Atlantic and (b) North Pacific along with the NAO and NPI indices (bold gray lines).

with each other ($r = 0.47$). The strongest disagreements between first PCs of h_w and h_s are observed during the 1960s, early 1970s, and the late 1980s. During the decades of the 1980s and 1990s correlation between the first PCs of wind sea and swell is somewhat higher than during the 1960s and 1970s. Moreover, during the first period SWH was more highly correlated with swell height, while during the last two decades SWH was largely dominated by the wind sea variability. In general, SWH is higher correlated with the wind sea than with the swell height. Correlation of the NAO index with SWH ($r = 0.81$) is higher than the correlation of the NAO index with individual wave components (sea and swell). Of these two components, wind sea is more strongly correlated with the NAO index than swell (Table 1).

The periods of 1958–79 and 1980–2002 are also characterized by strong differences in the level of correlation of the PCs of different wave components with NAO. Swell height is more closely correlated with the NAO index during the first period, while during the period of 1980–2002 wind sea demonstrates very close

TABLE 1. Correlation coefficients of the first normalized principal components of h_w, h_s, and SWH in the North Atlantic with each other and with the NAO index for different periods. All values are significant at the 99% level unless otherwise noted.

Periods pair of parameters	1958–2002	1958–79	1980–2002
h_w–h_s	0.47	0.44*	0.51*
h_w–SWH	0.82	0.75	0.89
h_s–SWH	0.74	0.79	0.72
h_w–NAO	0.68	0.50*	0.84
h_s–NAO	0.48	0.62	0.39**
SWH–NAO	0.81	0.83	0.79

* Significant at 95% level.
** Significant at 90% level.

correlation with NAO, with the swell being just loosely connected with NAO index. Jung et al. (2003) have described the NAO regime shift between the 1970s and 1980s in different atmospheric variables. Earlier, indications of the NAO shift manifestation in different atmospheric, oceanic, and ice characteristics were found by Kodera et al. (1999), Hilmer and Jung (2000), and Gulev et al. (2001, 2002). Gulev et al. (2001) and Chang (2004) found also that correlation between the North Atlantic and the North Pacific midlatitudinal storm tracks undergoes significant changes between the 1970s and 1980s. Table 1 establishes clear manifestations of the change in the NAO regime in the wind wave parameters in the North Atlantic.

Woolf et al. (2002) performed the EOF analysis of the altimeter SWH for 1985–99 using the data for the December–March period and obtained results very similar to our spatial patterns. Correlation of the first PC of SWH with NAO index was higher than 0.85. We reprocessed our data for the same months and time period and obtained a correlation coefficient between the first PC of SWH and NAO of 0.82. This indirectly demonstrates high comparability of SWH derived from VOS and altimeter data and shows that visual data are capable of demonstrating reliable variability patterns in SWH.

Figure 6b shows the time behavior of the winter PCs of wind sea heights, swell height and SWH in the North Pacific. Interannual variability of the winter SWH in the North Pacific is fully dominated by the swell variability. Their first normalized PCs are correlated with a correlation coefficient closely matching 1 (Table 2). Correlation between the first normalized PCs of wind sea and swell is somewhat higher than in the North Atlantic and also shows the strongest disagreement during the 1960s and a closer link during the last two decades. The strength of the North Pacific westerlies is characterized by the North Pacific Index (NPI) (Tren-

TABLE 2. Correlation coefficients of the first normalized principal components of h_w, h_s, and SWH in the North Pacific with each other and with NPI for different periods. All values are significant at the 99% level unless otherwise noted.

Periods pair of parameters	1958–2002	1958–79	1980–2002
h_w–h_s	0.56	0.36*	0.72
h_w–SWH	0.63	0.41**	0.78
h_s–SWH	0.98	0.99	0.98
h_w–NPI	0.72	0.63	0.76
h_s–NPI	0.58	0.33	0.75
SWH–NPI	0.61	0.37*	0.78

* Significant at 90% level.
** Significant at 95% level.

berth and Hurrell 1994), which is closely correlated with the first PC of the wind sea (Table 1). However, this correlation is considerably stronger during the period of 1980–2002 than during the decades of the 1960s and 1970s. Swell height and SWH show practically no correlation with NPI during the period of 1958–79, being highly correlated with NPI during the last two decades when the correlation coefficients for swell and SWH are as high as for the wind sea.

5. Association of wind wave variability with atmospheric circulation characteristics

Our analysis reveals the differences in temporal behavior of wind sea and swell along with different correlation levels between the leading modes of wind sea and swell with atmospheric circulation indices (NAO and NPI). In this context it is interesting to consider atmospheric circulation characteristics that might be responsible for the observed changes. Hogben (1995) first suggested a hypothetical qualitative mechanism though which wind sea and swell may show different interannual variability. He argued that an increase of storm frequency reduces the time of the swell decay between storms and provides a higher residual swell level, as an initial condition for the growth of newly generated young waves. This hypothesis associates swell variability primarily with the forcing frequency (occurrence of storms) and the wind sea changes with the forcing magnitude (wind speed). Gulev and Hasse (1999) found the evidence for this mechanism in the northeast Atlantic, using 30-yr time series of wind wave data (Gulev and Hasse 1998) and wind speed records at OWSs. On the other hand, Bauer et al. (1997) performed model experiments, artificially changing the storm frequency by reducing and enlarging the time resolution of surface winds, and did not find any evidence for the growing swells in the experiment with higher forcing frequency.

To analyze the connections between the variability in wind wave heights and atmospheric circulation characteristics during winter we used the detrended seasonal anomalies of surface wind speed and cyclone intensity over the Northern Hemisphere. Wind speed should reasonably well represent the local forcing, being responsible for the generation of the wind sea. We also hypothesize that the anomalies of cyclone numbers should effectively characterize the forcing frequency, quantifying the occurrence of storms. In particular, Weisse et al. (2005) argued that the number of severe and moderate storms experienced an increase in the northeast Atlantic during the last decades. We applied canonical correlation analysis (CCA) to the time series of wind speed, number of deep (<980 hPa) cyclones (nc), and wind wave height. CCA allows the pair of time series to retrieve the patterns that are optimally correlated with each other (von Storch and Zwiers 1999). The first five EOFs accounting for 69%–80% of the total variance in the wave fields in the Atlantic and for 63%–72% in the Pacific were used for the CCA. Table 3 shows canonical correlation coefficients between the first canonical patterns of wind speed and the number of deep cyclones, as well as wind sea height, swell height, and SWH. Remarkably, the highest canonical coefficients in the North Atlantic were obtained between the wind speed and wind sea height, and between the number of deep cyclones and swell height. They are higher than the canonical coefficients for the pairs nc–h_w and V–h_s and higher than the coefficients for SWH. Figure 7 shows the first canonical pairs of the wind speed and wind sea height as well as of the number of cyclones and swell height in the North Atlantic. The nc–h_s pair is represented by the maximum cyclone occurrence in the northeast Atlantic and Norwegian Sea, on the one hand, and by the swell pattern largely resembling its first EOF, on the other hand (Fig. 5). The pattern of the number of cyclones in the first canonical pair (Fig. 7a) in comparison to the first EOF of cyclone occurrence (Gulev et al. 2001) shows that the center of action is not in the subpolar North Atlantic between Greenland and Iceland, but in the northern European

TABLE 3. Canonical correlation coefficients for the first canonical pairs of wind speed, cyclone numbers, as well as wind sea, swell, and SWH. All values are significant at the 99% level unless otherwise noted.

Pair of parameters	North Atlantic	North Pacific
V–h_w	0.92	0.95
V–h_s	0.78	0.74
V–SWH	0.88	0.86
nc–h_w	0.71	0.79
nc–h_s	0.85	0.90
nc–SWH	0.83	0.87

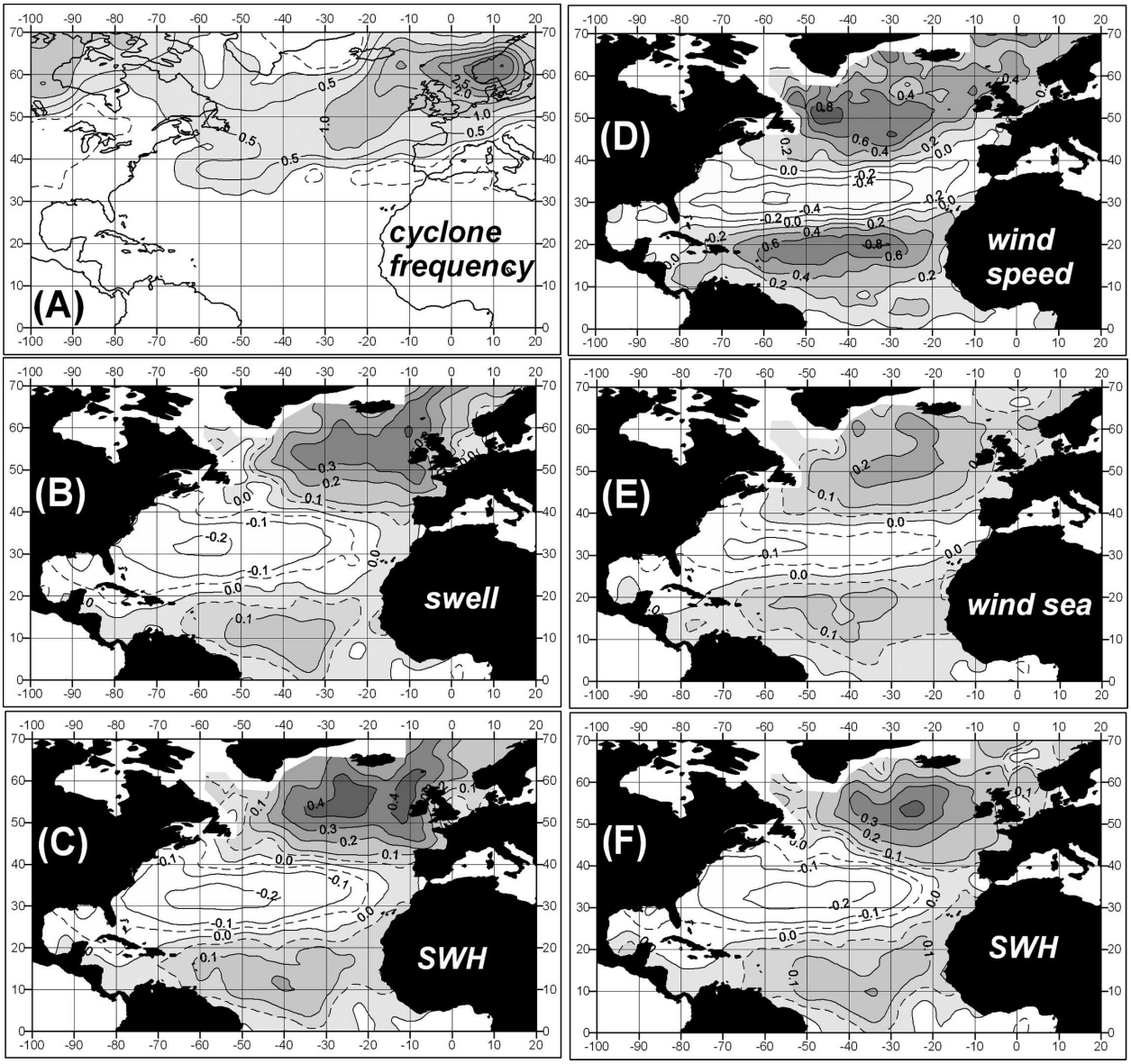

FIG. 7. Results of CCA for the North Atlantic. The first canonical pattern of the frequency of (a) deep cyclones (*n* per season per 5° box) and (b) swell height as well as canonical pattern of SWH, optimally correlated with the number of (c) deep cyclones. The first canonical pattern of the (d) wind speed and (e) wind sea height as well as canonical pattern of SWH, optimally correlated with the (f) wind speed.

basin and over Scandinavia. The increasing cyclone occurrence here results in the higher swells in the northeast Atlantic, as shown in Fig. 7b. The first canonical pair of the wind speed and wind sea height (Figs. 7d,e) is represented by the tripole patterns in both wind speed and wind sea height, with the latter being very close to the first EOF of the wind sea height. This pair reflects the importance of the local wind forcing for the interannual variability of the wind sea. Different roles of the forcing magnitude and forcing frequency in the variability of SWH is quite evident in Figs. 7c,f, showing the first canonical patterns of SWH and the number of cyclones (Fig. 7c) and wind speed (Fig. 7f). Their canonical counterparts (not shown) are very close to the patterns in Figs. 7a,d. The largest midlatitudinal anomalies of SWH forced by the local wind are observed in the central midlatitudinal Atlantic, being clearly associated with the wind sea variability. The highest anomalies driven by the cyclone frequency and associated with the swell variations are identified eastward in the northeast Atlantic and in the Norwegian Sea.

Figure 8 shows the results of the CCA in the North

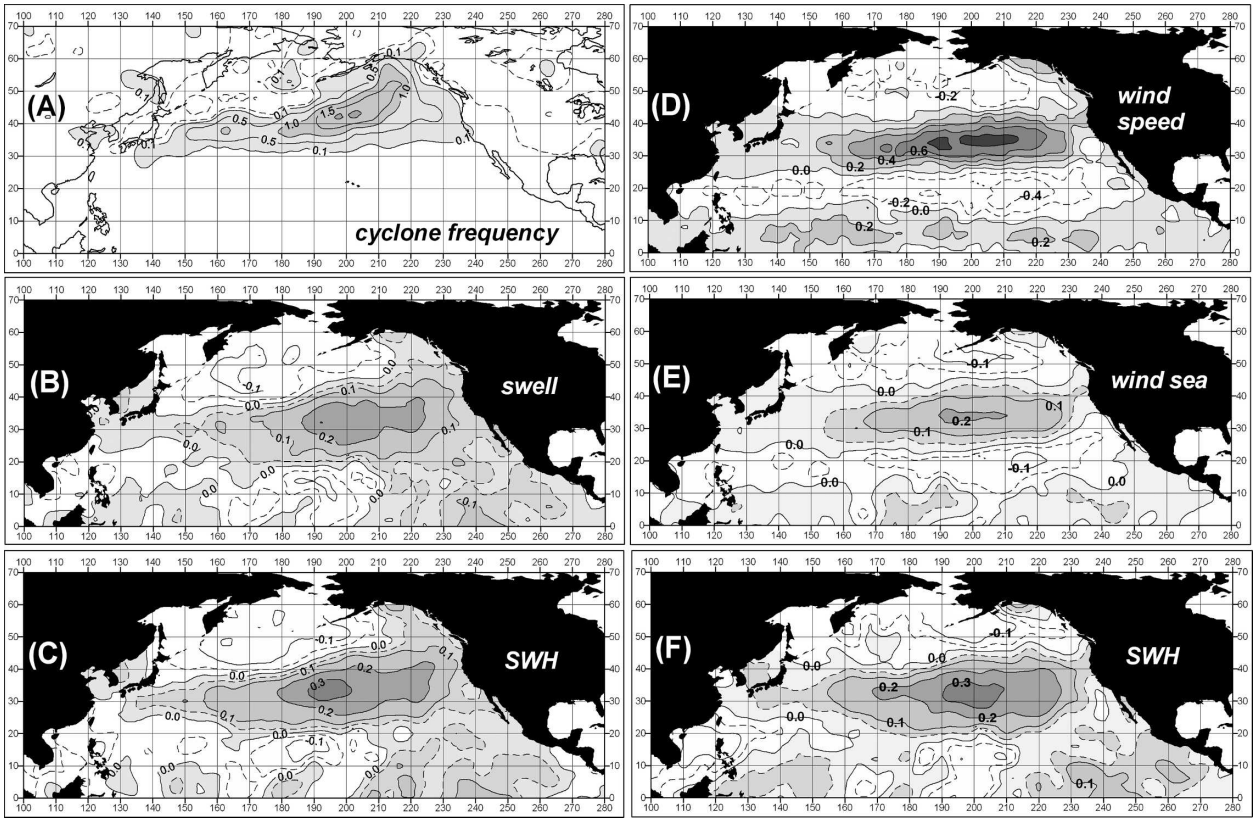

FIG. 8. Same as in Fig. 7, but for the North Pacific.

Pacific. The deep cyclone occurrence pattern in the first canonical pair nc–h_s is very close to the first EOF of cyclone numbers in the North Pacific (Gulev et al. 2001) with the main midlatitudinal storm track aligning from the southwest to the northeast and with the anomalies of the opposite sign in the northwest Pacific. The corresponding pattern of swell height is largely represented by the positive anomalies in the western Pacific midlatitudes and the negative anomalies in the eastern subpolar latitudes and Tropics. Although different from the first EOF of swell height in the Tropics, this pattern largely resembles the first EOF in the eastern midlatitudes, showing the largest anomalies at approximately 35°N and between 160°E and 180°. A canonical pair of the wind speed and wind sea height (Figs. 8d,e) is represented by the collocated tripole pattern with the subpolar, midlatitudinal, and tropical centers of action. This pattern in the mid- and subpolar latitudes resembles the first EOF of the wind sea height (Fig. 5d). The canonical counterparts of the cyclone occurrence and of the wind speed in the Pacific are represented by the patterns of swell and wind sea, which are much more consistent with each other than in the Atlantic. This is particularly evident in the canonical patterns of SWH with the number of deep cyclones (Fig. 8c) and wind speed (Fig. 8f), which are quite close to each other and demonstrate nearly the collocated patterns of the anomalies of one sign in midlatitudes and the opposite sign in the subpolar latitudes.

6. Summary and discussion

We analyzed the variability in the North Atlantic and North Pacific wind waves, swell, and SWH using 45 yr of VOS data, which provide separate estimates of the wind sea and swell heights. Patterns of secular changes and interannual variability of wind sea and swell demonstrate noticeable differences in the North Atlantic, being more consistent with each other in the Pacific. Trends in SWH in the northeast Atlantic primarily result from the swell changes and not from the wind sea, which shows weak negative trends here. Interannual time-scale variations of the wind sea and swell heights are highly correlated in the Pacific midlatitudes. However, in the Atlantic they are weakly linked to each other and imply that different mechanisms are responsible for the variability in wind sea and swell. To analyze potential mechanisms of the interannual variability of the wind sea and swell we considered the local forcing (wind speed) and storm frequency (quantified through the cyclone counts). To the extent that it is

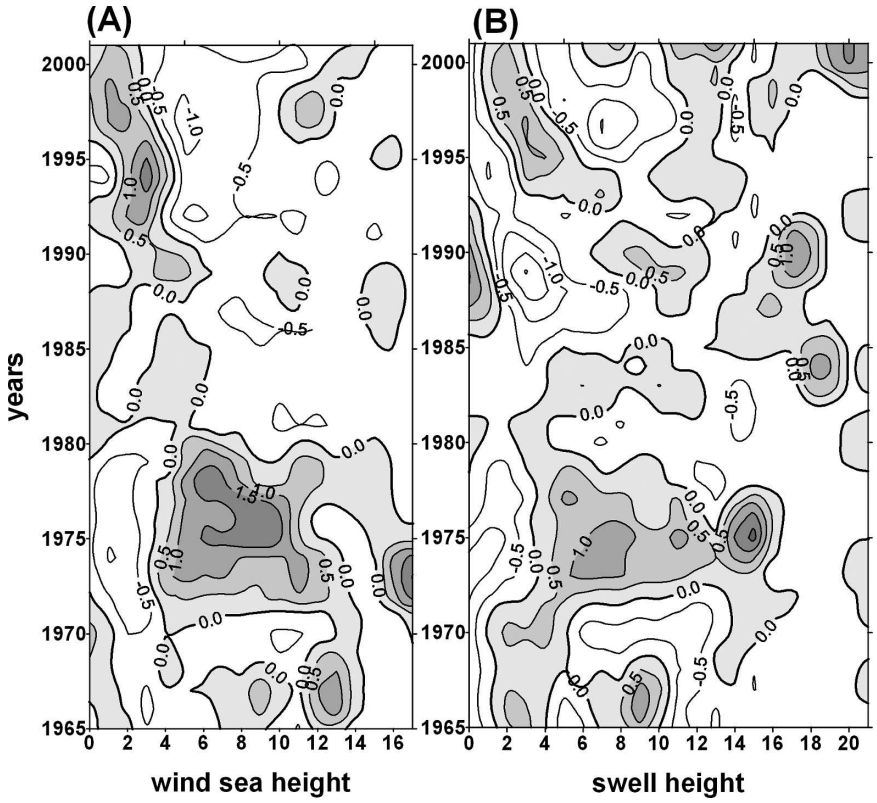

FIG. 9. Normalized occurrence anomalies of the winter wind (a) sea height and (b) swell height, smoothed with 3-yr RM for the area 50°–60°N, 10°–20°W in the Atlantic.

possible to make physical inferences from a purely statistical approach, we draw the conclusion that wind speed is a dominating factor in driving wind sea variability, while swell is primarily driven by the changes in cyclone counts. The resulting variations in SWH, at least in the North Atlantic, are more controlled by variability in swell than in the wind sea. This implies that they are also controlled by cyclone activity, which is closely associated with the swell changes.

Our conclusions were drawn on the basis of VOS data, which are the only providers of independent estimates of wind sea and swell. Demonstrated differences in the wind sea and swell leading modes of variability put more light on the nature of changes in SWH that are typically analyzed in the model studies (Sterl and Caires 2005; Wang and Swail 2002; and others). At least in the northeast Atlantic and to some extent in the northeast Pacific these changes can be largely attributed to the variations in swell height, rather than to the wind sea. However, wind sea causes much of the danger for the operations of marine carriers, except for very large tankers and container ships, which can also suffer from the high swells even under calm conditions. Moreover, swell significantly affects the tankers approaching the oil platforms for bunkering. The mechanism behind the cyclone frequency impact on the changes in swell and therefore in SWH (Hogben 1995; Gulev and Hasse 1999) implies association with the number of deep cyclones in the northeast Atlantic with the swell changes. Gulev et al. (2001) have demonstrated the growing number of deep cyclones in the North Atlantic and their close association with the NAO index. This is consistent with the growing number of severe storms in the northeast Atlantic (Weisse et al. 2005). For the 10° × 10° box 50°–60°N, 10°–20°W we derived the occurrence histograms of wind sea height and swell height for individual winters. Then they were transformed into occurrence anomalies around the averaged over observational period probability density distribution. Then the anomalies were normalized by scaling with interannual standard deviations (std) of the occurrence for the selected bins,

$$P'(x) = \frac{P(x) - \overline{P}(x)}{\sigma[P(x)]}, \tag{2}$$

where x is the analyzed wave parameter (e.g., wind sea/swell height or SWH), $P(x)$ is probability density distribution for an individual winter, $P'(x)$ is the normalized anomaly of the probability density distribution, and the overbar stands for the averaging operator. In

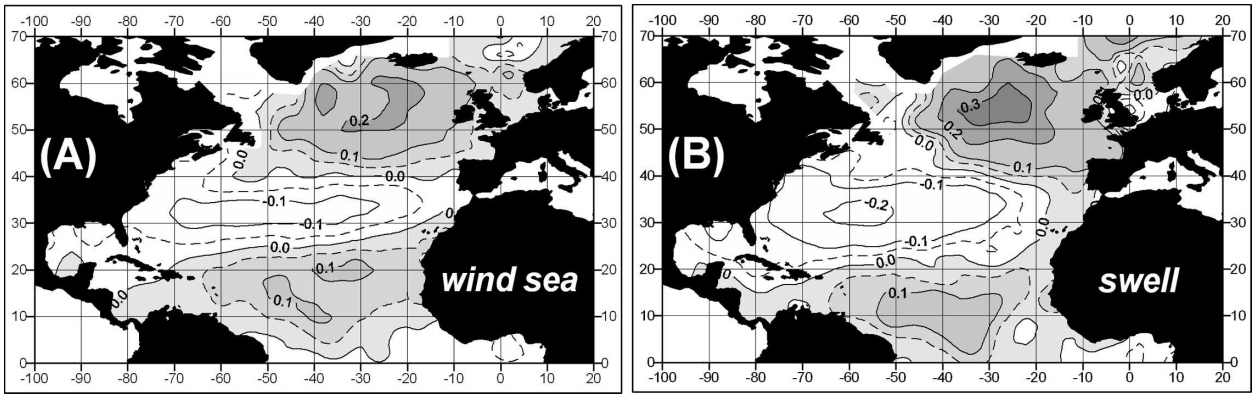

FIG. 10. The first canonical patterns of the winter wind (a) sea height and (b) swell height in the North Atlantic.

Fig. 9 we show these normalized occurrence anomalies smoothed with 3-yr running mean for the period after 1963. Although for the period before 1963 the total number of ICOADS reports in this area is just 2 times smaller than for the later decades, they are largely represented by the reports from the OWSs I (59°N, 19°W) and J (52.5°N, 20°W), located on the western boundary of the box. This could result in the regional sampling bias in statistical distributions. Remarkably, Fig. 9a shows a decreasing occurrence of high wind seas. In the 1960s and 1970s positive anomalies are observed for the classes of wind sea height from 4 to 14 m, while in the 1980s and 1990s positive occurrence anomalies are primarily observed for the small wind seas (less than 4 m). At the same time, the occurrence anomalies for the classes of high swells (Fig. 9b) are primarily positive during the last two decades, implying a growing probability of the high swells during the observational period.

An alternative explanation of different variability patterns of wind sea and swell (Figs. 7, 8) can be that the swell propagates to the northeast from the area of the strongest wind sea changes and this propagation results in the pattern of swell variability shifted to the northeast. However, the canonical correlation coefficients between wind sea and swell are even slightly lower than between wind speed and swell, being 0.73 in the North Atlantic and 0.70 in the North Pacific. Moreover, the first canonical patterns of wind sea and swell (Fig. 10) show practically the collocated maxima of the explained variance in the central midlatitudinal Atlantic. Figure 10 shows that for the changes in swell heights the propagation mechanism can be probably as important as the cyclone impact in the Norwegian Sea, where wind sea and swell demonstrate weak anomalies of the opposite sign. However, in the northeast Atlantic there is no indication of the downstream shift of the swell pattern with respect to the wind sea to the extent implied by Fig. 7. Similar analysis performed for the North Pacific (no figure shown) demonstrates even more consistent wind sea and swell canonical patterns than in the North Atlantic. For the 10° box in the northeast Atlantic (50°–60°N, 10°–20°W) where swell variability can be hypothesized to originate from the wind sea variability southwestward, we performed directional analysis of the swell time series. Table 4 shows the correlation coefficients between the mean winter swell height and the height of swells propagating from different directions. The highest correlation of 0.63 is obtained for the swells propagating from the northwest, implying that swells coming from this sector largely determine the mean swell in the region. The correlation coefficient for the swells propagating from the southwest is considerably smaller (0.41). This does not support the hypothesis that swell variability in the northeast Atlantic originates from wind seas southwestward.

Our results should be considered in a view of reliability of visual wave data. Analysis of trends may be influenced by inhomogeneity of sampling, especially prior to 1963, when the number of wave reports was 2–3 times smaller than in the later decades. Inadequate sampling may result in both random and nonrandom (potentially associated with the fair weather bias) uncertainties (Gulev et al. 2003a). We used the ERA-40 WAM 6-hourly wave hindcast (Sterl and Caires 2005) and subsampling methodology of Gulev et al. (2003a) for estimation of sampling errors. For the period of 1958–63 sampling errors were higher than for the later decades in 1.5–1.7 times in the North Atlantic and in 1.3–1.6 times in the North Pacific. Analysis of trends for the period from 1963 to 2002 shows that in the North Atlantic trends are very close to those computed for the whole period. In the North Pacific trends for the two periods are in qualitative agreement, being quantitatively 10%–20% smaller in the northwest Pacific midlatitudes. Over most of the North Atlantic and North

TABLE 4. Correlation coefficients between the total mean swell height in the 10° box at 50°–60°N, 10°–20°W and the mean heights of swells propagating from different directional sectors. All values are significant at the 99% level unless otherwise noted.

Directional sector	Correlation with the mean swell height	No. of observations (%)
Southwest	0.41	41
Northwest	0.63	39
Southeast	0.28*	11
Northeast	0.42	9

* Significant at 95% level.

Pacific no statistically significant differences between the trends for the two periods were identified. For the two regions shown in Fig. 2 trends in wind sea became slightly stronger during the period of 1963–2002 compared to 1958–2002 (respectively, −11.7 versus −10.3 cm decade^{-1} in the Atlantic and 14.1 versus 13.3 cm decade^{-1} in the Pacific). Trends in swell and SWH became alternatively weaker (respectively, 18.3 versus 21.2 cm decade^{-1} in the Atlantic and 16.2 versus 21.1 cm decade^{-1} in the Pacific), being significant at the same level.

Locally negative trends in wind sea in the northeast Atlantic (Figs. 1a, 2a) should generally imply also negative trends in the wind speed. However, as was pointed out above, estimation of wind speed trends in VOS data is highly uncertain. We derived estimates of linear trends for this northeast Atlantic region (Fig. 2a) from the NCEP–NCAR reanalysis and ICOADS data for different types of wind observations in VOS (Table 5). Reanalysis winds report positive changes that are consistent with the estimates obtained from VOS, if all wind observations are used. This agreement is not surprising because reanalysis assimilated raw VOS observations (Kalnay et al. 1996). However, if we consider only the VOS reports containing wave information (VOS_*W* in Table 5) the linear trend becomes weakly negative and insignificant (Table 5). This may partly reflect the fair weather bias. We can note at this point, that our analysis and results of Kent and Taylor (1995) do not show significant changes in the major routes during severe weather. Typically, ships tend to slow down, though remaining on the same route and thus continue to report on Global Telecommunication System (GTS). The time series constructed from only Beaufort estimates of wind speed (VOS_*WB* in Table 5) show an already negative trend that is significant at the 90% level. To provide comparability we recomputed wind sea trends using only VOS_*WB* reports and obtained a negative trend of −0.12 m decade^{-1}, which is very close to that shown in Fig. 2a. Linear trends derived from all wind speed reports after correction of anemometer heights (*VOS_WC* in Table 5) are still weakly negative but not significant. However, we could properly apply this correction only for the period of availability of the WMO-47 document (Kent et al. 2006) after 1973, using the default heights for the earlier years. Thus, the impact of anemometer measurements on wind speed time series may imply positive trends in the wind speed.

TABLE 5. Linear trends in the NCEP–NCAR and VOS wind speed [(m s^{-1}) decade^{-1}] estimated for the area 56°–64°N, 10°–20°W in the North Atlantic. Estimates "VOS" were derived from all VOS reports with wind speed; "VOS_*W*" from only the reports containing wave information; "VOS_*WB*" from only those of "VOS_*W*," which reported Beaufort estimates of wind speed; "VOS_*WC*" from the reports containing wave information with the correction of anemometer winds.

Wind speed product	Linear trend in wind speed [(m s^{-1}) decade^{-1}]
NCEP–NCAR	0.17*
VOS	0.14**
VOS_*W*	−0.02
VOS_*WB*	−0.07**
VOS_*WC*	−0.04

* Significant at 95% level.
** Significant at 90% level.

Isemer (1995) compared linear trends in ocean wind speed derived from homogeneous data from OWSs and the VOS in the vicinity of OWSs. For the period from the late 1940s to early 1970s, data from OWS I in this region reveal a significantly negative trend, while VOS data do not show any significant changes. For the period from the mid-1970s to the late 1980s OWS L, located approximately 200 km from OWS L, reports negative changes of 0.4 m s^{-1} decade^{-1}, while VOS data report a significantly positive trend of 0.24 m s^{-1} decade^{-1}. To obtain longer-term estimates time series from both OWS I and L can be considered together (e.g., Gulev et al. 2000). Analysis of the merged time series also shows a negative trend significant at the 90% level in the OWS wind data and an insignificantly positive trend in VOS data for the period of 1958–94. These results were also confirmed by the analysis of the upper-air data from radiosonde records (Isemer 1995). Ward (1992) and Ward and Hoskins (1996) have also shown that the northeast Atlantic trends in the wind speed demonstrate disagreement with the alternative estimates derived from the pressure gradient data.

Reliability of changes identified in wind sea and swell heights may be influenced by the uncertainties of separation of wind sea and swell in the VOS data. On the one hand, a two-step methodology of separation (Gulev et al. 2003a), based on the analysis of "wave height–wind speed" diagrams overplotted by the Joint North

Sea Wave Observation Project (JONSPAP) curves for different wind durations (Carter 1982) and wave age analysis, should guarantee a clear separation of wind sea and swell and identify the reports in which young swells are reported as wind seas or mature wind seas are reported as swells. On the other hand, Gulev et al. (2003b), analyzing the questionnaire distributed among VOS officers, argued that frequently (15%–30%) observers report wind sea height based on wind observations and thus provide a simplified wind-based wave hindcast. However, this practice was not the case for the swell height. Thus, we can argue that our results are not strongly influenced by the uncertainty of separation between wind sea and swell in the VOS data. Moreover, poor separation of wind sea and swell can only alternatively mask the effect shown in Figs. 1, 5, and 7 and not to lead to such an effect.

Future analysis of variability of wind sea, swell, and SWH on the basis of VOS data should go in the direction of the tendencies in extreme wave heights, which are the most dangerous for marine structures. Wang and Swail (2001) and Caires and Sterl (2005a) reported growing extreme SWH in wave model hindcasts driven by the reanalysis winds from the 1960s to the 1990s. This allowed Wang et al. (2004) to project the changes in SWH onto the twenty-first century. To test this hypothesis using the VOS data characterized by inhomogeneous time and space sampling (Gulev et al. 2003a) is not an easy task. Application of the peak-over-threshold (POT) method (Caires and Sterl 2005b) to the regularly sampled model data is quite different from the case when the data are characterized by numerous gaps as in the case with the VOS reports. Nevertheless, recently Anderson et al. (2001) developed a methodology to be used for satellite data, which are also undersampled, being however much more homogeneous than the VOS data. Further development of this methodology and its application to the VOS data will make it possible to derive for the first time VOS-based extreme wave statistics not only for SHW, but also separately for wind sea and swell. Given the importance of separate consideration of highest wind seas and swells, mentioned above, this will be a very challenging task of wave climate research and marine engineering.

Acknowledgments. We greatly appreciate support of Steve Worley of NCAR (Boulder, Colorado) and Scott Woodruff of NOAA CDC (Boulder, Colorado) in the access to the ICOADS marine reports database. We thank Andreas Sterl and Sofia Caires of KNMI (De Bilt, Netherlands), David Woolf and Peter Challenor of SOC (Southampton, United Kingdom), Vincent Cardone and Andrew Cox of Ocean Weather, Inc. (Cos Cob, Connecticut), Val Swail of Environment Canada (Toronto, Ontario, Canada), Hans-Joerg Isemer of GKSS (Geesthacht, Germany), and Irina Rudeva and Olga Zolina of IORAS (Moscow, Russia) for the useful discussions on different aspects of this work. Suggestions and criticism of two anonymous reviewers seriously helped to improve the manuscript. This study is supported by the EU-INTAS Grant 02-2206 and by Russian Ministry of Education and Science under the "World Ocean Federal Programme." SKG benefited also from the support of the Deutsche Forschungsgemeinschaft Sonderforschungsbereich SFB-460.

REFERENCES

Akima, H., 1970: A new method of interpolation and smooth curve fitting based on local procedures. *J. Assoc. Comput. Mach.,* **17,** 589–602.

Allan, J. C., and P. D. Komar, 2000: Are ocean wave heights increasing in the Eastern North Pacific. *Eos, Trans. Amer. Geophys. Union,* **81,** 561–566.

Anderson, C. W., D. J. T. Carter, and P. D. Cotton, 2001: Wave climate variability and impact on offshore design estimates. Shell International and the Organization of Oil and Gas Producers Rep., 99 pp.

Bacon, S., and D. J. T. Carter, 1991: Wave climate changes in the North Atlantic and North Sea. *Int. J. Climatol.,* **11,** 545–588.

——, and ——, 1993: A connection between mean wave height and atmospheric pressure gradient in the North Atlantic. *Int. J. Climatol.,* **13,** 423–436.

Barratt, M. J., 1991: Waves in the North East Atlantic. HMSO, U.K. Department of Energy Report OTI 90545, 16 pp. plus 40 figs.

Bauer, E., and C. Staabs, 1998: Statistical properties of global significant wave height and their use for validation. *J. Geophys. Res.,* **103,** 1153–1166.

——, M. Stolley, and H. von Storch, 1997: On the response of surface waves to accelerating the wind forcing. GKSS Manuscript 96/E/89, 24 pp.

Bromirski, P. D., R. E. Flick, and D. R. Cayan, 2003: Storminess variability along the California coast: 1858–2000. *J. Climate,* **16,** 982–993.

Caires, S., and V. Swail, 2004: Global wave climate trend and variability analysis. *Proc. Eighth Int. Workshop on Wave Hindcasting and Forecasting,* Oahu, HI, U.S. Army Engineer Research and Development Center's Coastal and Hydraulics Laboratory and Cosponsors, CD-ROM, Al.

——, and A. Sterl, 2005a: 100-year return value estimates for wind speed and significant wave height from the ERA-40 data. *J. Climate,* **18,** 1032–1048.

——, and ——, 2005b: A new nonparameteric method to correct model data: Application to significant wave height from the ERA-40 Re-Analysis. *J. Atmos. Oceanic Technol.,* **22,** 443–459.

Cardone, V. J., J. G. Greenwood, and M. A. Cane, 1990: On trends in historical marine wind data. *J. Climate,* **3,** 113–127.

Carter, D. J. T., 1982: Prediction of wave height and period for a constant wind velocity using the JONSWAP results. *Ocean Eng.,* **9,** 17–33.

——, and L. Draper, 1988: Has the North-East Atlantic become rougher? *Nature,* **332,** 494.

Challenor, P., and P. D. Cotton, 2003: The joint calibration of altimeter and in-situ wave heights. *Advances in Applications of Marine Climatology,* WMO, 139–148.

Chang, E. K. M., 2004: Are the Northern Hemisphere winter storm tracks significantly correlated? *J. Climate,* **17,** 4230–4244.

Cotton, P. D., P. G. Challenor, L. Redbourn-Marsh, S. K. Gulev, A. Sterl, and R. S. Bortkovskii, 2003: An intercomparison of voluntary observing, satellite data and modeling wave climatologies. *Advances in Applications of Marine Climatology,* WMO, 127–138.

Cox, A. T., and V. R. Swail, 2001: A global wave hindcast over the period 1958-1997: Validation and climatic assessment. *J. Geophys. Res.,* **106,** 2313–2329.

Dacunha, N. M. C., N. Hogben, and K. S. Andrews, 1984: Wave climate synthesis worldwide. *Proc. Int. Symp. on Wave and Wind Climate Worldwide,* London, United Kingdom, Royal Institute of Naval Architects, 1–11.

da Silva, A. M., C. C. Young, and S. Levitus, 1994: *Anomalies of Directly Observed Quantities*. Vol. 2, *Atlas of Surface Marine Data 1994,* NOAA, Atlas NESDIS 7, 416.

Duchon, C. E., 1979: Lanczos filtering in one and two dimensions. *J. Appl. Meteor.,* **18,** 1016–1022.

Gower, J. F. R., 2002: Temperature, wind and wave climatologies, and trends from marine meteorological buoys in the northeast Pacific. *J. Climate,* **15,** 3709–3718.

Graham, N., and H. Diaz, 2001: Evidence for intensification of North Pacific winter cyclones since 1948. *Bull. Amer. Meteor. Soc.,* **82,** 1869–1883.

Grigoriev, S., S. K. Gulev, and O. Zolina, 2000: Software for storm tracking and atmospheric cyclone analysis. *Eos, Trans. Amer. Geophys. Union,* **81,** 170–171.

Gulev, S. K., 1999: Comparison of COADS Release 1a winds with instrumental measurements in the North Atlantic. *J. Atmos. Oceanic Technol.,* **16,** 133–145.

——, and L. Hasse, 1998: North Atlantic wind waves and wind stress fields from voluntary observing data. *J. Phys. Oceanogr.,* **28,** 1107–1130.

——, and ——, 1999: Changes of wind waves in the North Atlantic over the last 30 years. *Int. J. Climatol.,* **19,** 1091–1117.

——, and V. Grigorieva, 2004: Last century changes in ocean wind wave height from global visual wave data. *Geophys. Res. Lett.,* **31,** L24302, doi:10.1029/2004GL021040.

——, P. D. Cotton, and A. Sterl, 1998: Intercomparison of the North Atlantic wave climatology from in-situ, voluntary observing, satellite data and modelling. *Phys. Chem. Earth,* **23,** 587–592.

——, O. Zolina, and Y. Reva, 2000: Synoptic and subsynoptic variability in the North Atlantic as revealed by the Ocean Weather Station data. *Tellus,* **52A,** 323–329.

——, ——, and S. Grigoriev, 2001: Extratropical cyclone variability in the Northern Hemisphere winter from the NCEP/NCAR Reanalysis data. *Climate Dyn.,* **17,** 795–809.

——, T. Jung, and E. Ruprecht, 2002: Interannual and seasonal variability in the intensities of synoptic-scale processes in the North Atlantic midlatitudes from the NCEP–NCAR reanalysis data. *J. Climate,* **15,** 809–828.

——, V. Grigorieva, A. Sterl, and D. Woolf, 2003a: Assessment of the reliability of wave observations from voluntary observing ships: Insights from the validation of a global wind wave climatology based on voluntary observing ship data. *J. Geophys. Res.,* **108,** 3236, doi:10.1029/2002JC001437.

——, ——, K. M. Selemenov, and O. Zolina, 2003b: Evaluation of surface winds and waves from voluntary observing ship data. *Advances in Applications of Marine Climatology,* WMO, 53–67.

Günther, H., W. Rosenthal, M. Stawarz, J. C. Carretero, M. Gomez, I. Lozano, O. Serano, and M. Reistad, 1998: The wave climate of the Northeast Atlantic over the period 1955-94: The WASA wave hindcast. *Global Atmos. Ocean Syst.,* **6,** 121–163.

Hayashi, Y., 1982: Confidence intervals of a climatic signal. *J. Atmos. Sci.,* **39,** 1895–1905.

Hilmer, M., and T. Jung, 2000: Evidence for a recent change in the link between the North Atlantic Oscillation and Arctic sea ice. *Geophys. Res. Lett.,* **27,** 989–992.

Hogben, N., 1988: Experience from compilation of Global Wave Statistics. *Ocean Eng.,* **15,** 1–31.

——, 1995: Increases in wave heights over the North Atlantic: A review of the evidence and some implications for the naval architect. *Trans. Roy. Inst. Nav. Archit.,* **137A,** 93–115.

——, and F. E. Lumb, 1967: *Ocean Wave Statistics*. HMSO, 263 pp.

——, and M. J. Tucker, 1994: Sea-state development during severe storms: Assessment of data and case histories. *Underwater Technol.,* **20,** 23–31.

——, N. M. C. Dacunha, and K. S. Andrews, 1983: Assessment of a new global capability for wave climate synthesis. *Proc. OCEAN'83,* San Francisco, CA, IEEE, 1–6.

——, ——, and G. F. Oliver, 1986: *Global Wave Statistics*. Unwin Brothers, 661 pp.

Houmb, O. G., K. Mo, and T. Overvik, 1978: Reliability tests of visual wave data and estimation of extreme sea states. Division of Port and Ocean Engineering, University of Trondheim, Norwegian Institute of Technology Rep. 5, 28 pp.

Hurrell, J. W., 1995: Decadal trends in the North Atlantic Oscillation: Regional temperatures and precipitation. *Science,* **269,** 676–679.

Isemer, H.-J., 1995: Trends in marine surface wind speed: Ocean Weather Stations versus Voluntary Observing Ships. *Proc. Int. COADS Winds Workshop,* Kiel, Germany, NOAA and IFM, 68–84.

Jardine, T. P., 1979: The reliability of visually observed wave heights. *Coastal Eng.,* **3,** 33–38.

Josey, S., E. K. Kent, and P. K. Taylor, 1999: New insights into the ocean heat budget closure problem from analysis of the SOC air-sea flux climatology. *J. Climate,* **12,** 2856–2880.

Jung, T., M. Hilmer, E. Ruprecht, S. Kleppek, S. K. Gulev, and O. Zolina, 2003: Characteristics of the recent eastward shift of interannual NAO variability. *J. Climate,* **16,** 3371–3382.

Kalnay, E., and Coauthors, 1996: The NCEP/NCAR 40-Year Reanalysis Project. *Bull. Amer. Meteor. Soc.,* **77,** 437–471.

Kent, E. C., and P. K. Taylor, 1995: A comparison of sensible and latent heat flux estimates for the North Atlantic Ocean. *J. Phys. Oceanogr.,* **25,** 1530–1549.

——, and ——, 1997: Choice of a Beaufort equivalent scale. *J. Atmos. Oceanic Technol.,* **14,** 228–242.

——, C. D. Woodruff, and D. I. Berry, 2006: WMO publication no. 47: Metadata and an assessment of observational heights in ICOADS. *J. Atmos. Oceanic Technol.,* in press.

Kistler, R., and Coauthors, 2001: The NCEP–NCAR 50-Year Reanalysis: Monthly means CD-ROM and documentation. *Bull. Amer. Meteor. Soc.,* **82,** 247–267.

Kodera, K., H. Kolde, and H. Yoshimura, 1999: Northern Hemisphere winter circulation associated with the North Atlantic Oscillation and stratospheric polar night jet. *Geophys. Res. Lett.,* **26,** 443–446.

Korevaar, C. G., 1990: *North Sea Climate Based on Observations from Ships and Lightvessels*. Kluwer Academic, 137 pp.

Kushnir, Y., V. J. Cardone, J. G. Greenwood, and M. A. Cane, 1997: The recent increase in the North Atlantic wave height. *J. Climate,* **10,** 2107–2113.

Laing, A. K., 1985: An assessment of wave observations from ships in Southern Ocean. *J. Climate Appl. Meteor.,* **24,** 481–494.

Lanczos, C., 1956: *Applied Analysis*. Prentice-Hall, 539 pp.

Lindau, R., 1995: A new Beaufort equivalent scale. *Proc. Int. COADS Winds Workshop,* Kiel, Germany, NOAA and IFM, 232–252.

——, 2006: The elimination of spurious trends in marine wind data using pressure observations. *Int. J. Climatol.,* **26,** 797–817.

——, H.-J. Isemer, and L. Hasse, 1990: Towards time-dependent calibration of historical wind observations at sea. *Trop. Ocean-Atmos. Newslet.,* **54,** 7–12.

Murray, R. J., and I. Simmonds, 1991: A numerical scheme for tracking cyclone centres from digital data. Part I: Development and operation of the scheme. *Aust. Meteor. Mag.,* **39,** 155–166.

Naval Oceanography Command Detachment, 1981: *US Navy Marine Climatic Atlas of the World*. 169 pp.

Neu, H. J. A., 1984: Interannual variations and longer-term changes in the sea state of the North Atlantic from 1970 to 1982. *J. Geophys. Res.,* **89,** 6397–6402.

Paskausky, D., J. D. Elms, R. G. Baldwin, P. L. Franks, C. N. Williams, and K. G. Zimmerman, 1984: Addendum to wind and wave summaries for selected U.S. Coast Guard operating areas. NCDC NOAA, 523 pp.

Peterson, E. W., and L. Hasse, 1987: Did the Beaufort scale or the wind climate change? *J. Phys. Oceanogr.,* **17,** 1071–1074.

Ramage, C. S., 1984: Can shipboard measurements reveal secular changes in tropical air–sea heat flux?. *J. Climate Appl. Meteor.,* **23,** 187–193.

Rodewald, M., 1972: Long-term variations of the sea temperature in the area of the nine North Atlantic Ocean Weather Stations during the period 1951-1968. *Rapp. P. V. Reun. ICES,* **162,** 139–153.

Rye, H., 1976: Long-term changes in the North Sea wave climate and their importance for the extreme wave predictions. *Mar. Sci. Commun.,* **2,** 420–488.

Schmidt, H., and H. von Storch, 1993: German bight storms analysed. *Nature,* **370,** 791.

Soares, C. G., 1986: Assessment of the uncertainty in visual observations of wave height. *Ocean Eng.,* **13,** 37–56.

Sterl, A., 2004: On the (in)homogeneity of reanalysis products. *J. Climate,* **17,** 3866–3873.

——, and S. Caires, 2005: Climatology, variability and extrema of ocean waves—The Web-based KNMI/ERA-40 wave atlas. *Int. J. Climatol.,* **25,** 963–977.

——, G. J. Komen, and D. Cotton, 1998: 15 years of global wave hindcasts using ERA winds: Validating the reanalysed winds and assessing the wave climate. *J. Geophys. Res.,* **103,** 5477–5492.

Swail, V., A. Cox, and V. Cardone, 1999: Trends and potential biases in NCEP-driven ocean wave hindcasts. *Proc. Second Int. Conf. on Reanalyses,* Reading, United Kingdom, WMO Tech. Doc. 985/WCRP-109, 129–132.

Trenberth, K. E., and J. W. Hurrell, 1994: Decadal atmosphere-ocean variations in the Pacific. *Climate Dyn.,* **9,** 303–319.

Uppala, S. M., and Coauthors, 2005: The ERA-40 re-analysis. *Quart. J. Roy. Meteor. Soc.,* **131,** 2961–3012.

Vikebo, F., T. Furevik, G. Furnes, N. G. Kvamst, and M. Reistad, 2003: Wave height variations in the North Sea and on the Norwegian Continental Shelf, 1881–1999. *Cont. Shelf Res.,* **23,** 251–263.

von Storch, H., and F. W. Zwiers, 1999: *Statistical Analysis in Climate Research*. Cambridge University Press, 503 pp.

Walden, H., N. Hogben, M. D. Burkhart, R. Dorrestein, W. H. Warnsink, and Y. Yamanouchi, 1970: Long term variability. *Proc. Fourth Int. Ship Structure Congress,* Report of Committee 1, Tokyo, Japan, 49–59.

Wang, X. L., and V. R. Swail, 2001: Changes of extreme wave heights in Northern Hemisphere oceans and related atmospheric circulation regimes. *J. Climate,* **14,** 2204–2221.

——, and ——, 2002: Trends of Atlantic wave extremes as simulated in a 40-yr wave hindcast using kinematically reanalyzed wind fields. *J. Climate,* **15,** 1020–1035.

——, and ——, 2006: Historical and possible future changes of wave height in Northern Hemiphere oceans. *Atmosphere-Ocean Interactions,* W. Perrie, Ed., Vol. 2, Wessex Institute of Technology Press, 185–218.

——, F. W. Zwiers, and V. R. Swail, 2004: North Atlantic Ocean wave climate change scenarios for the twenty-first century. *J. Climate,* **17,** 2368–2383.

Ward, M. N., 1992: Provisionally corrected surface wind data, worldwide ocean-atmosphere surface fields, and Sahelian rainfall variability. *J. Climate,* **5,** 454–475.

Ward, N. M., and B. J. Hoskins, 1996: Near surface wind over the Global Ocean 1949-1988. *J. Climate,* **9,** 1877–1895.

WASA Group, 1998: Changing waves and storms in the Northeast Atlantic? *Bull. Amer. Meteor. Soc.,* **79,** 741–760.

Weisse, R., H. von Storch, and F. Feser, 2005: Northeast Atlantic and North Sea storminess as simulated by a regional climate model 1958-2001 and comparison with observations. *J. Climate,* **18,** 465–479.

Wilkerson, J. C., and M. D. Earle, 1990: A study of differences between environmental reports by ships in the voluntary observing program and measurements from NOAA buoys. *J. Geophys. Res.,* **95,** 3373–3385.

WMO, 1970: The Beaufort scale of wind force. Rep. 3, Reports on Marine Science Affairs, 22 pp.

——, 1973: International list of selected, supplementary and auxiliary ships. WMO-47.

Wolter, K., 1997: Trimming problems and remedies in COADS. *J. Climate,* **10,** 1980–1997.

Woolf, D. K., P. G. Challenor, and P. D. Cotton, 2002: Variability and predictability of North Atlantic wave climate. *J. Geophys. Res.,* **107,** 3145, doi:10.1029/2001JC001124.

——, P. D. Cotton, and P. Challenor, 2003: Measurements of the offshore wave climate around the British isles by satellite altimeter. *Philos. Trans. Roy. Soc. London,* **361A,** 27–31.

Worley, S. J., S. D. Woodruff, R. W. Reynolds, S. J. Lubker, and N. Lott, 2005: ICOADS release 2.1 data and products. *Int. J. Climatol.,* **25,** 823–842.

Zolina, O., and S. K. Gulev, 2002: Improving accuracy of mapping cyclone numbers and frequencies. *Mon. Wea. Rev.,* **130,** 748–759.